# Cooperativity during the Formation of Peptide/MHC Class II Complexes†

Matthew W. Anderson and Jack Gorski*

*Blood Research Institute, Blood Center of Southeastern Wisconsin, Milwaukee, Wisconsin 53201, and Department of Microbiology and Molecular Genetics, Medical College of Wisconsin, Milwaukee, Wisconsin 53201*

*Received June 24, 2004; Revised Manuscript Received February 15, 2005*

ABSTRACT: To generate an effective immune response, class II major histocompatibility complex molecules (MHCII) must present a diverse array of peptide ligands for recognition by T lymphocytes. Peptide/MHCII complexes are stabilized by hydrophobic anchoring of peptide side chains to pockets in the MHCII protein and the formation of hydrogen bonds to the peptide backbone. Many current models of peptide/MHCII association assume an additive and independent contribution of the interactions between major MHCII pockets and corresponding side chains in the peptide. However, significant conformational rearrangements occur in both the peptide and MHCII during binding. Therefore, we hypothesize that peptide binding to MHCII could be viewed as a folding process in which both molecules cooperate to produce the final conformation. To directly test this hypothesis, we adapt a serial mutagenesis strategy to study cooperativity in the interaction of the human MHCII HLA-DR1 and a peptide derived from influenza hemagglutinin. Substitutions in either the peptide or HLA-DR1 that are predicted to interfere with hydrogen bond formation show cooperative effects on complex stability and affinity. Substitution of a peptide side chain that provides a hydrophobic contact also contributes to the cooperative effect, suggesting a role for all energetic sources in the folding process. We propose that cooperativity throughout the peptide-binding groove reflects the folding of segments of the MHCII molecule into helices around the peptide with a concomitant folding of the peptide into a polyproline helix. The implications of cooperativity for peptide/MHCII structure and epitope selection are discussed.

MHC class II molecules (MHCII)[1] are heterodimeric glycoproteins that present antigenic peptides to T lymphocytes in order to initiate or propagate an immune response. Selection of peptide via the MHCII pathway (epitope selection) involves a series of molecular and cellular events within specialized cells of the immune system (*1*). Initially, MHCII $\alpha/\beta$ heterodimers are synthesized bound to a chaperone molecule called invariant chain, which targets the complex to the endosomal compartment, an active site of antigen degradation. In this low pH, protease-rich environment, the invariant chain molecule is cleaved, freeing MHCII to bind antigenic peptide in a process influenced by the peptide-exchange protein HLA-DM (*2*). Crystallographic analysis of peptide/MHCII complexes has identified two major sources of binding energy (*3*): one is the sequestration of peptide side chains or "anchors" in polymorphic pockets in the MHCII protein, and the second is the formation of a hydrogen bond (H-bond) network between main chain atoms of the peptide and conserved residues in the MHCII. Through the use of single amino acid substitutions in the peptide (*4*, *5*) or randomly generated peptide libraries (*6*), complementary side chain/pocket interactions at the major pockets P1, P4, P6, and P9 have been identified as critical for peptide binding to MHCII. Viewed from this perspective, the peptide/MHCII interaction is a docking event mediated by the anchoring side chains. Side chain/pocket "motifs" have been useful in identifying potential T cell epitopes (*7*), yet fail to explain those instances of high affinity peptide/MHCII interactions in the absence of major anchor/pocket interactions (*8*−*10*). In addition, we have recently observed that multiple substitutions in "minor" anchor positions P2, P3, P7, and P10 can reduce the affinity ($K_D$) of the $HA_{306-318}$ (HA) peptide ligand for the human MHCII HLA-DR1 (DR1) over 11000-fold, despite the fact that the "major" anchor/pocket interactions remained unchanged (*11*).

An important limitation of the "anchor/pocket" model of peptide/MHCII binding is the assumption that the contribution to binding energy by either the peptide or MHCII is additive and independent (*12*, *13*). However, we prefer to consider the formation of a peptide/MHCII complex as an example of a folding interaction, a view that has been suggested previously (*14*). Such a model would be compatible with an increasing appreciation of the role of conformational flexibility in molecular recognition (*15*), especially for proteins involved in the immune response (*16*). Indeed, peptide/MHCII complexes exhibit significant conformational flexibility as shown by at least two conformational states: an "open," or "active" fast dissociating conformer, and a "closed" or "compact", kinetically stable conformer (*17*−*22*). These conformers are involved in peptide binding to MHCII, as kinetic studies reveal a fast bimolecular peptide/MHCII association step to generate the open conformer,

† This work was supported by NIH Grant RO1AI26085.

* To whom correspondence should be addressed. Mailing address: The Blood Center of Southeastern Wisconsin, P.O. Box 2178, Milwaukee, WI 53201. Tel: 414-937-6367. Fax: 414-937-6284. E-mail: jack@bcsew.edu.

[1] Abbreviations: MHCII, major histocompatibility complex II; DR1, HLA-DR1; PBS, phosphate-buffered saline; H-bond, hydrogen bond; HA, hemagglutinin; wt, wild-type.

10.1021/bi048675s CCC: $30.25 
Published on Web 03/25/2005

followed by a slower unimolecular conformational change step to produce the stable complex (*23*−*25*). Furthermore, these conformational changes are dependent on the nature of the peptide ligand (*19*, *26*, *27*), and may act as a "kinetic trap" to increase the longevity and presentation of peptide/MHCII complexes (*18*, *25*). Peptide binding may also trigger global conformational changes in the MHCII protein, including regions in the MHCII $\beta$ chain distal to the peptide binding groove (*28*).

As a consequence of the folding process, conformational changes in proteins are often characterized by measurable cooperativity between functional subunits (*29*). Therefore, one would predict that peptide binding to MHCII would be a highly cooperative process. Although experiments specifically designed to test for cooperativity in peptide/MHCII interactions have not been reported, some studies have noted possible cooperative effects on peptide affinity and stability among anchor/pocket interactions in MHC class I (*30*) and MHCII (*31*) molecules, and H-bonds in peptide/MHCII complexes (*32*). However, the relationship between peptide/MHCII folding and cooperativity remains unclear.

In this work we utilize multiple, iterative amino acid substitutions in the complex of the HA peptide and DR1 in an attempt to identify and quantify cooperative interactions between peptide and MHCII. First, we analyze a series of substitutions that are positioned across the binding groove that do not influence the primary hydrophobic anchor interactions, and are predicted to either directly or indirectly destabilize the H-bond network. In keeping with significant conformational changes occurring in the MHCII upon complex formation, we find cooperative effects on peptide dissociation and binding. We extend these observations to include the effect of changing a side chain involved in weak hydrophobic anchoring, indicating that all energetic sources can contribute to cooperativity. Finally, we propose that cooperativity is directly related to the conversion from the open to closed conformer of the peptide/MHCII complex, a transition that is dependent on the conformational changes that accompany folding.

## MATERIALS AND METHODS

*Peptide Synthesis*. Peptides derived from the sequence GPKYVKQNTLKLAT, representing residues 306−318 of the hemagglutinin protein from influenza A virus (H3 subtype), are described in Table 1. The N-terminal Gly facilitated labeling. Side chains in the HA peptide are numbered relative to the P1 Tyr residue (*33*). Peptides were synthesized by standard solid-phase methods, purified by HPLC, and confirmed by mass spectrometry. N-Terminal labeling with FITC (Molecular Probes) or LC-LC biotin (Pierce) was performed on the resin before deprotection, and then peptides were cleaved and purified as above.

*Expression and Purification of Recombinant Soluble HLA-DR1 Protein*. Recombinant soluble empty (peptide-free) DR1 was produced and immunoaffinity purified from a stably transfected *Drosophila* S2 insect cell line essentially as described (*34*). Purity was confirmed by SDS−PAGE, and protein was concentrated using centrifugal ultrafiltration (Amicon). DR1 protein was quantified by measuring the UV absorbance at 280 nm using an $E_{280}$ of 56340 $M^{-1}$ $cm^{-1}$. DR1 protein was buffer exchanged into PBS (7 mM $Na^+$/$K^+$ phosphate, 135 mM NaCl, pH 7.4) before use.

Table 1: Affinity and Dissociation Rate of Substituted Peptide/HLA-DR1 Complexes

| complex | $K_D$ (nM) | $t_{1/2}$ (min) |
|---|---|---|
| $\beta$81/HA 306−318 | 50.6 ± 2 | 3971 ± 244 |
| $\beta$81/P7 L→P | 64.4 ± 2 | 3187 ± 48 |
| $\beta$81/P2 V→S | 75.2 ± 4 | 2712 ± 198 |
| DR1/HA 306−318 | 85.3 ± 3 | 3974 ± 255 |
| DR1/P2 V→S | 97.2 ± 4 | 3378 ± 101 |
| DR1/P7 L→P | 102.4 ± 7 | 3704 ± 82 |
| $\beta$81/P10 A→G | 118.4 ± 5 | 2048 ± 56 |
| $\beta$81/P2,7 VL→SP | 132.9 ± 13 | 1664 ± 75 |
| DR1/P2,7 VL→SP | 140.2 ± 9 | 2288 ± 56 |
| DR1/P10 A→G | 157.9 ± 6 | 3821 ± 265 |
| $\beta$81/P7,10 LA→PG | 184.6 ± 10 | 1546 ± 111 |
| DR1/P7,10 LA→PG | 225.0 ± 14 | 3296 ± 141 |
| DR1/P3 K→D | 318.9 ± 12 | 2834 ± 215 |
| DR1/P2,10 VA→SG | 373.1 ± 15 | 970 ± 151 |
| $\beta$81/P2,10 VA→SG | 558.5 ± 67 | 589 ± 59 |
| DR1/P2,7,10 SPG | 605.3 ± 40 | 753 ± 150 |
| $\beta$81/P3 K→D | 643.9 ± 36 | 1307 ± 222 |
| DR1/P3,7 KL→DP | 684.7 ± 50 | 1542 ± 144 |
| $\beta$81/P2,7,10 SPG | 1174 ± 66 | 378 ± 27 |
| $\beta$81/P3,7 KL→DP | 2481 ± 265 | 604 ± 34 |
| DR1/P2,3 VK→SD | 3568.9 ± 67 | 667 ± 50 |
| DR1/P3,10 KA→DG | 4818.7 ± 187 | 551 ± 66 |
| $\beta$81/P2,3 VK→SD | 9170 ± 945 | *a* |
| DR1/P3,7,10 DPG | 9991.9 ± 917 | *a* |
| DR1/P2,3,7 SDP | $13.3 \pm 1.3 \times 10^3$ | *a* |
| $\beta$81/P3,10 KA→DG | $14.0 \pm 1.7 \times 10^3$ | *a* |
| $\beta$81/P2,3,7 SDP | $33.4 \pm 1.5 \times 10^3$ | *a* |
| $\beta$81/P3,7,10 DPG | $35.4 \pm 2.7 \times 10^3$ | *a* |
| DR1/P2,3,10 SDG | $88.9 \pm 3.2 \times 10^3$ | *a* |
| $\beta$81/P2,3,10 SDG | $26.1 \pm 1.0 \times 10^4$ | *a* |
| DR1/P2,3,7,10 SDPG | $31.3 \pm 0.7 \times 10^4$ | *a* |
| $\beta$81/P2,3,7,10 SDPG | $78.1 \pm 5.9 \times 10^4$ | *a* |

[a] Not done.

*Generation and Expression of $\beta$81 Substituted HLA-DR1 Molecules*. Plasmids encoding truncated forms of the HLA-DR$\alpha$ and DR$\beta$*(0101) genes were the gift of Dr. Lawrence Stern (U. Mass. Medical School). Position 81 His of the $\beta$ chain was substituted to Asn through the use of the QuikChange site-directed mutagenesis kit (Stratagene) and the primer 5′:CCAACCCCGTAGTTGTTTCTGCAGTAG-GTGTC:3′. The mutation was confirmed by sequencing, and wild-type (wt) $\alpha$ and mutant $\beta$ plasmids were cotransfected into *Drosophila* S2 cells. Stable transfectants were selected and grown in the presence of 25 $\mu$g/mL blasticidin (Invitrogen). $\beta$81 substituted DR1 ($\beta$81) protein was expressed and purified as for the wt protein. SDS−PAGE analysis of purified $\beta$81 and wtDR1 proteins revealed no significant differences in migration or purity.

*Native PAGE Analysis of Peptide Dissociation*. DR1/peptide complexes were formed by incubating 1 $\mu$M DR1 protein with a 10-fold molar excess of FITC-labeled peptide in 50 mM $NaH_2PO_4$ and 50 mM sodium citrate (pH 5.3) and protease inhibitors for 16 h at 37 °C. DR1/peptide complexes were then purified from unbound labeled peptide by buffer exchange into PBS with a Centricon-30 spin filter that had been preincubated with 25 mM MES (pH 6.5). Purified DR1/peptide complexes were then quantified by reading the UV absorbance at 280 nm, factoring in an $E_{280}$ of 1280 $M^{-1}$ $cm^{-1}$ for the Tyr residue and 10846 $M^{-1}$ $cm^{-1}$ for the fluorescein present in the bound peptide. Purified DR1/peptide complexes (85 nM) were then incubated with 10 $\mu$M unlabeled HA peptide at 37 °C in 50 mM $NaH_2PO_4$ and 50 mM sodium citrate (pH 5.3). To prevent nonspecific

adherence of the protein, siliconized tubes were used. At various timepoints, aliquots of the reaction were removed and quenched with 0.5 M Tris-HCl (pH 8.0) in gel loading buffer and immediately placed on ice. The aliquots were then loaded onto a 5/12% native PAGE gel (Biorad) and quickly separated by electrophoresis at 150 V for 30 min. FITC-peptide/DR1 complexes were then visualized using a FluorImager (Molecular Dynamics). Data was normalized and expressed as the % of FITC-peptide/DR1 complex remaining relative to the complex at $t = 0$, and fit to a single-exponential model ($y = ae^{-bx}$). Each experiment was performed in triplicate, and the reported dissociation rate reflects the mean ± SD of two independent experiments.

*Competitive Peptide Binding Assay*. Relative binding affinities were determined by a competitive binding assay essentially as described (*35*). DR1 or $\beta$81 protein (4 nM) was incubated with 4 nM biotinylated HA peptide in PBS (0.1% BSA, 0.01% Tween 20, 0.1 mg/mL 4-(2-aminoethyl)-benzene sulfonyl fluoride 0.1 mM iodoacetamide, 5 mM EDTA, 0.02% $NaN_3$, pH 7.2) in the presence of varying amounts of inhibitor peptides for 3 days at 37 °C. The incubation time ensures that the majority (>65%) of DR1 protein participates in the peptide binding reaction to reach equilibrium (*25*). Bound biotinylated peptide was detected using a solid-phase immunoassay and $Eu^{2+}$ labeled streptavidin. Plates were read using a Wallac VICTOR counter (PerkinElmer Wallac). Data was fit to a logistic equation $\{y = a/[1 + (x/x_0)^b]\}$. $IC_{50}$ values were obtained from the curve fit of the binding data and converted to $K_D$ values by using the equation $K_D = (IC_{50})/(1 + ([bHA]/K_{D,bHA}))$, in which $K_{D,bHA}$ was set equal to 17.7 nM or 8.5 nM on the basis of the results of the direct binding of bio-HA peptide to wtDR1 or $\beta$81, respectively (data not shown). Each point represents the mean and SD of three independent experiments. Because peptide/MHCII binding represents a multistep reaction, the $IC_{50}$ for a competitive binding assay may not be directly proportional to the $K_D$ (*36*). While this can be offset by long incubations relative to half-life, we study low affinity peptides where half-lives are impossible to determine. Therefore, the values of affinity reported herein should be considered as apparent $K_D$ values.

*Calculation of Cooperative Effect*. We view cooperativity in peptide/MHCII folding as the enhancement in binding or dissociation that arises in a second (or subsequent) interaction as a result of the primary interaction. This definition has been used by others in the context of protein folding (*37*) or ligand binding (*38*). We utilized a multiple substitution strategy previously used to identify interacting partners during protein folding (*39*, *40*). To normalize the $t_{1/2}$ and $K_D$ values of a given peptide/MHCII complex, we define the effect of each substitution as the ratio of the substituted measurement over that of the wtDR1/HA value ($\Delta t_{1/2}$ for stability or $\Delta K_D$ for affinity). Normalization of the measurements to that of the wtDR1/HA complex also allows for comparison of cooperativity measures in stability, which is measured directly, and affinity, which is measured indirectly.

For calculating cooperativity, the effect of multiple substitutions ($\Delta t_{1/2,obs}$ $x,y$) or ($\Delta K_{D,obs}$ $x,y$) is measured directly. The expected value ($\Delta t_{1/2,exp}$) ($\Delta K_{D,exp}$) for a combination of substitutions (i.e. $x$ and $y$) is calculated as the product of the individual substitutions [e.g. $\Delta t_{1/2,exp}$ $x,y = (\Delta t_{1/2}, x) \times (\Delta t_{1/2}, y)$]. For peptides with three or more substitutions, the expected value would be the product of all the different substitutions [e.g. $\Delta t_{1/2,exp}$ $x,y,z = (\Delta t_{1/2}, x) \times (\Delta t_{1/2}, y) \times (\Delta t_{1/2}, z)$]. The cooperativity is the ratio of the expected to observed ($C$ = exp/obs) values for either $\Delta t_{1/2}$ or $\Delta K_D$. A value of 1 for the ratio of expected/observed $\{[(\Delta t_{1/2,exp}\ x,y)/(\Delta t_{1/2,obs}\ x,y)]$ or $[(\Delta K_{D,exp}\ x,y)/(\Delta K_{D,obs}\ x,y)] = 1\}$ indicates no cooperativity. Cooperativity is evidenced when the ratio of expected/observed is not equal to 1. Errors were calculated using standard error propagation techniques in which the relative error (error/value) of the final calculation is the sum of all the relative errors involved in the calculation.

## RESULTS

*Substitution Strategy*. The binding of the influenza HA peptide to DR1 has been extensively characterized, and the complex represents one of the first peptide/MHCII structures generated (*33*). We have recently shown that multiple substitutions across the peptide binding groove at P2, P3, P7, and P10, representing solvent accessible residues that do not interact with the major hydrophobic pockets, can reduce affinity of the peptide for DR1 over 11000-fold (*11*). Structural modeling revealed that three of these substitutions could potentially interfere with formation of H-bonds normally observed in the HA/DR1 structure (Figure 1, red circles). The P2 Ser and P3 Asp substitutions are located at positions in the peptide/DR1 interface in which rotation of the side chain around the α-carbon can directly destabilize H-bonds to the peptide backbone. Alternatively, these substitutions may indirectly lead to destabilization by facilitating solvent entry into the binding groove. The P10 Gly substitution may also indirectly disrupt H-bonds by allowing increased solvent access to the C-terminal end of the peptide binding groove in a manner similar to that observed in the HLA-DR4/Col II structure (*41*). Indeed, use of a solvent that helps destabilize H-bonds increased the effect of substitutions at these positions (*11*).

As previous work suggested that H-bonds disproportionately contribute to the stability of peptide/MHCII complexes (*32*, *42*), we hypothesized that multiple disruptions to the H-bond network through these peptide side chain substitutions could lead to cooperative effects on complex stability. In addition to the P2, P3, and P10 substitutions in the HA peptide we included a substitution at position $\beta$81 of the DR1 molecule. This substitution can disrupt a H-bond to the main chain carbonyl oxygen of the P(−1) peptide residue (Figure 1, violet circle) (*32*, *42*). This experimental approach yielded 11 different complexes with two or more substitutions.

*Cooperativity in Complex Stability*. To evaluate the effect of these substitutions on the kinetic stability of the peptide/DR1 complex, dissociation rate data was obtained (Figure 2A). The $t_{1/2}$ values for the various complexes are reported in Table 1. While each individual substitution resulted in small to negligible effects on the dissociation rate (<1.4-fold), multiple substitutions had significantly larger effects (i.e. 7-fold for the $\beta$81/P2,10 complex). This large increase in dissociation rate in the presence of multiple substitutions suggested a cooperative effect. To investigate this possibility, the effect of each singly substituted (P2, P3, P10, or $\beta$81) complex was calculated with respect to the stability of the unsubstituted DR1/HA complex. If the contribution of each

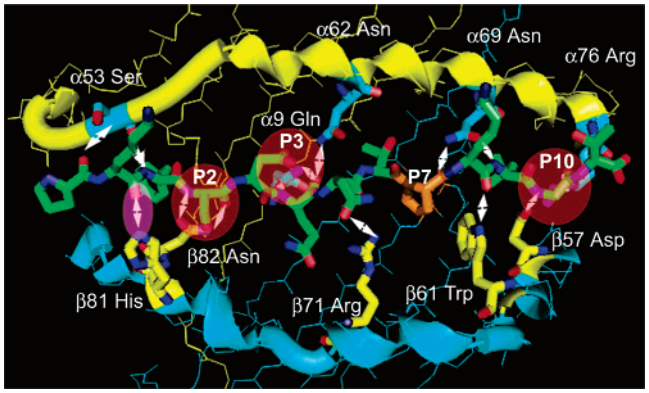


FIGURE 1: Substitutions in the HLA-DR1/HA complex to analyze cooperative interactions between peptide and MHCII. The DR1 molecule complexed to a fully substituted HA peptide is shown with H-bonds designated as white arrows. The α-chain is in yellow, the *β*-chain in blue, and the peptide in green. The peptide substitutions of solvent accessible side chains that are postulated to directly or indirectly disrupt the H-bond network, P2, P3, and P10, are highlighted in red. The H-bond between *β*81 His and the carbonyl of P(−1), which is disrupted by the *β*81 His to Asn substitution, is highlighted in violet. The substitution at P7 of Leu to Pro is highlighted orange. The P2 Val to Ser substitution would affect H-bonds between *β*82 Asn and the P2 amide and carbonyl groups. The P3 substitution, Lys to Asp, is postulated to destabilize the H-bonds between α9 Gln (partially hidden below the peptide) and α62 Asn with the carbonyl of P4. The substitution at P10, Val to Gly, is postulated to disrupt the H-bond between *β*57 Asp and the P10 amide as well as a postulated H-bond between α76 and the P10 carbonyl. The P2 and P3 substitutions can either disrupt the H-bonds directly, by assuming a rotamer in which the side chain can compete with the backbone for the MHCII side chain, or, in the case of P3 Asp, possibly bind to the peptide backbone itself. Disruption by the P10 substitution is postulated to arise from increased solvation at the end of the groove, due to the loss of the methyl group. Solvent effects may also play a role in the P2 and P3 substitutions. The P7 Leu to Pro substitution affects hydrophobic interactions at this minor pocket in the DR1 structure (*43*, *44*) decreasing the contact surface. As can be seen, all the H-bond interactions except for α9 Gln arise from interactions with side chains originating from the most exposed regions of the MHCII, large sections of which are folded into helices in the crystal structure. Coordinates taken from ref *51* were modified using Swiss PDB Viewer (*52*). The model was generated using PyMol (*53*).

substitution to complex stability was independent (i.e. no cooperativity), then the effect of multiple substitutions should equal the product of their individual effects on stability (see Materials and Methods). For example, the reduction in complex stability by the P3 K→D substitution was 1.4-fold, while the effect of the *β*81 substitution was negligible (1.0). Therefore, the expected value for their combined effect should be about 1.4-fold (1.4 × 1.0). In contrast, the *β*81/P3 K→D double substituted complex resulted in a 3-fold reduction in complex stability (Figure 2B). The data suggest that contributions to binding energy from both the peptide and MHCII are important in generating the final complex. Furthermore, the magnitude of the cooperative effect increased exponentially as a function of complex stability. Plotting the cooperativity values and $t_{1/2}$ for each multisubstituted complex on a ln scale (Figure 2C) revealed a linear relationship with a negative slope (−0.84), reflecting the negative cooperativity we measure. Because of the poor binding properties of some of the multisubstituted complexes, dissociation rate data could only be obtained for 7 of the 11 possible complexes.

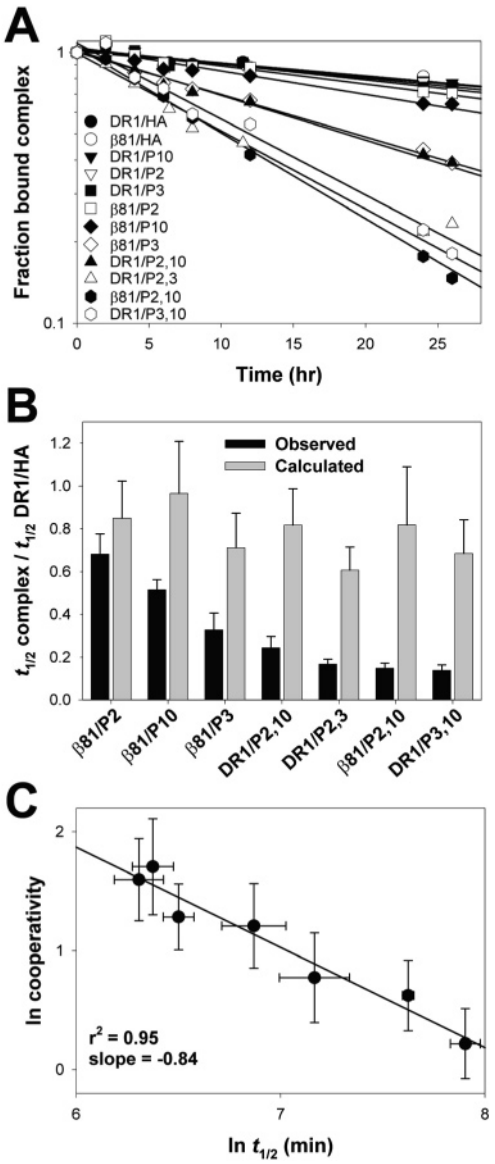


FIGURE 2: Cooperativity in peptide/MHCII dissociation. (A) Dissociation rates of wild-type HLA-DR1 (DR1) or *β*81 substituted DR1 (*β*81)/peptide complexes were measured as described in Materials and Methods. Data are expressed as the fraction FITC-peptide/MHCII complex remaining relative to $t = 0$. Reactions were performed in triplicate, and data series represent one of two independent experiments. The lines represent the fit of the data to a single-exponential function. $t_{1/2}$ values are as reported in Table 1. (B) The observed ratio (black bars) of $t_{1/2}$ values for each peptide/MHCII complex as compared to the $t_{1/2}$ of the DR1/HA complex is plotted alongside the calculated $t_{1/2}$ ratio (gray bars) for each complex assuming an independent effect of each substitution. Error bars were calculated by standard error propagation techniques. (C) Natural log (ln) plot of cooperativity (expected/observed $t_{1/2}$) vs dissociation rate for each peptide/MHCII complex tested. Horizontal error bars represent the SD of the $t_{1/2}$ measurement. Vertical error bars represent the error of the cooperativity as calculated through standard error propagation. The line indicates the fit of the data to a linear regression.

*Cooperativity in Peptide Affinity*. Although the measurement of $t_{1/2}$ as described above provided a direct measure of the cooperativity in the dissociation rate of the multisubstituted complexes, it would also be informative to determine if cooperative effects would be observed in the affinity of the various complexes. Peptide affinity was measured using an equilibrium-based competition-binding assay in which

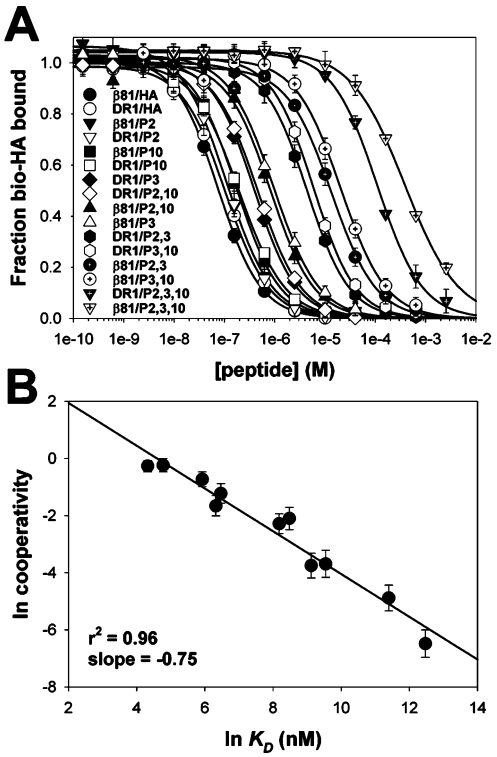


FIGURE 3: Cooperativity in peptide affinity for MHCII. (A) Competitive binding analysis of P2, P3, and P10 substituted HA peptide variants to either DR1 or $\beta$81. Data represents the mean and SD of three independent experiments. Lines indicate the fit of the data to a logistic equation. $K_D$ values are as reported in Table 1. (B) Natural log (ln) plot of cooperativity (expected/observed $K_D$) vs $K_D$ for each peptide/MHCII complex tested. Error bars are as described for Figure 2C. The line indicates the fit of the data to a linear regression.

each peptide was tested for its ability to compete against the HA peptide for binding to either wtDR1 or $\beta$81 molecules. This enabled the examination of cooperative effects in highly unstable multisubstituted complexes in which dissociation rate data was difficult to obtain. The competition data for all eleven multisubstituted complexes is shown in Figure 3A, and the $K_D$ values are reported in Table 1. To quantify cooperative effects on peptide affinity, a calculation similar to that done previously with the dissociation rate data was performed. In this case, the effect of each substitution was compared to the $K_D$ of the unsubstituted DR1/HA complex, and the calculated effect of multiple substitutions was obtained. By plotting cooperativity (expected/observed) against the observed $K_D$ of each complex, we again observed an exponential relationship with cooperativity increasing as peptide affinity decreased (Figure 3B). The relationships between cooperativity and either $K_D$ or $t_{1/2}$ were very similar (slope $-0.75$ vs $-0.84$ respectively), suggesting that the cooperative effects measured were fundamental to the peptide/DR1 interaction and not due to an artifact of the particular assay system used.

*Contribution of a Hydrophobic Interaction to the Cooperative Effect.* A previous report had noted a possible cooperative effect between hydrophobic pocket/anchor interactions in MHCII (*31*). We asked whether substitution at a position involved predominantly in a hydrophobic interaction could contribute to the cooperative effect we observed with substitutions that were predicted to impact the H-bond network. To investigate this possibility, we used a Leu to Pro substitution at P7 to affect hydrophobic/van der Waals interactions at this shallow pocket/shelf in the DR1 structure (Figure 1) (*43*). Analysis of this substitution in a peptide/DR1 structure (*44*) indicates that the contact surface is decreased with the Pro at this position, as the Leu fits into the shallow pocket under the $\beta$-chain helix while the Pro occupies the center of the groove. As shown in Figure 4A, dissociation rate data was obtained for substituted DR1/HA complexes which contained a Pro substitution at P7. The $t_{1/2}$ values for these complexes are reported in Table 1. Cooperativity was calculated as described previously and plotted against the observed stability of the complex on a ln scale. As shown in Figure 4B, we found that the overall relationship of the cooperative effect to the dissociation rate was very similar for those complexes with and without Pro at P7, suggesting that substitution of a hydrophobic interaction could also contribute to cooperative effects mediated by direct or indirect H-bond disruption. The exponential rise in the cooperative effect was maintained with a small change in slope, $-0.88$ vs. $-0.84$ (Figure 2C).

To determine if the Pro substitution at P7 would exhibit similar effects on cooperativity in affinity, we determined the $K_D$ of P7 substituted complexes (Figure 4C). Similar to the result obtained by dissociation rate determination, we found a high correlation between cooperativity and $K_D$ for those complexes that did and did not contain a Pro at P7 (Figure 4D) with a small change in the overall slope of the relationship, $-0.77$ vs $-0.75$ (Figure 3B). It should be pointed out that not all P7 Pro substituted peptides showed cooperativity as there is a cluster of five points close to zero (Figure 4D). These predominantly represent peptides with the P7 Pro and one other substitution. Taken together, these results strongly suggested that all sources of binding energy available to the peptide and MHCII could be used to mediate cooperative effects in peptide/MHCII interactions.

## DISCUSSION

Despite evidence of conformational change during formation of peptide/MHCII complexes, most models of the peptide/MHCII interaction assume that a few ligand/receptor interactions (anchors/pockets) act independently of each other to provide the majority of the binding energy. This has translated into epitope recognition algorithms in which the independent interaction of various allele-specific pockets with corresponding peptide side chains are used to predict binding (*12*, *13*). We prefer to consider peptide binding to MHCII and the conformational change implicit in the interaction as a folding problem. To understand the impact of conformational change on the outcome of peptide/MHCII interactions, we utilized a multiple substitution approach to evaluate whether binding energy from both the peptide and MHCII could cooperate in producing the final conformation. By substituting side chains in either the HA peptide or DR1, we show the presence of cooperative effects on complex stability and affinity. Furthermore, cooperative effects could be observed between substitutions which affect the H-bond network and those which affect hydrophobic anchoring, suggesting that both types of binding energy can mediate the conformational change in peptide/MHCII, a result in agreement with previous studies of peptide-induced conformational changes in DR1 (*27*). Finally, cooperative effects between contributions to binding energy by both the peptide

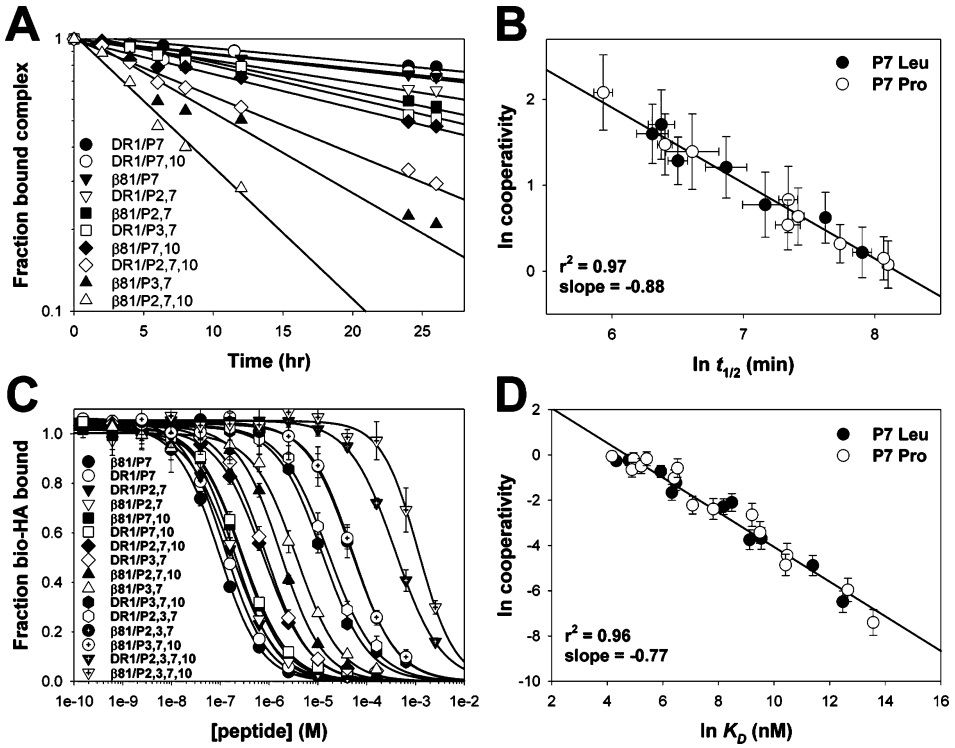


FIGURE 4: Effect of hydrophobic interactions on peptide/MHCII cooperativity. (A) Dissociation rate of complexes containing a P7 L→P substitution from DR1 and $\beta$81 molecules. Data is plotted as described in Figure 2A. (B) Natural log (ln) plot of cooperativity vs dissociation rate for HA peptides containing Leu at P7 (closed circles) or Pro at P7 (open circles). Error bars are as described in Figure 2C. The line indicates the fit of the data to a linear regression. (C) Competitive-binding analysis of peptides containing a P7 L→P substitution. Data is plotted as described in Figure 3A. (D) Natural log (ln) plot of cooperativity vs $K_D$ for peptides containing Leu at P7 (closed circles) or Pro at P7 (open circles). Error bars are as described in Figure 2C. The line indicates the fit of the data to a linear regression.

and DR1 support the concept that peptide/MHCII binding represents a concerted, bimolecular folding event (*14*).

During the folding process, the peptide/MHCII interaction can be considered as transitioning between two states: an open conformer from which peptide release is rapid, and the closed conformer which represents the stable complex. We view the open state as a folding intermediate in which the $\alpha$1/$\beta$1 helical regions of the MHCII molecule remain partially disordered. In this model, the cooperativity we observe can be visualized as a progressive folding of the partially unfolded and flexible helical regions onto the peptide, with each productive peptide/MHCII interaction influencing the next. Complete folding of the helices through interactions with the peptide during binding results in the stable, closed conformer. Concomitant with the folding of the MHCII $\alpha$1/$\beta$1 helices is the folding of the peptide into a polyproline type II conformation, which is conserved in all peptide/MHCII structures studied to date (*3*). Interestingly, many of the H-bonds that stabilize the binding and conformation of the peptide originate from MHCII side chains that are in the helices. Although formation of the H-bond network has been viewed in terms of stabilizing the peptide, it is likely to play a similar role for the $\alpha$1/$\beta$1 helices. While Trp, His, and Asn are infrequently observed in $\alpha$ helical regions in globular proteins (*45*), in MHCII they are frequently found making contributions to the H-bond network formed between the peptide and the $\alpha$1/$\beta$1 $\alpha$ helical domains. For example, $\beta$61 Trp is within an $\alpha$ helical segment, but by forming a H-bond to the P8 peptide main chain carboxyl (Figure 1) the local $\alpha$ helical conformation of the $\beta$1 domain can be stabilized. Through similar mechanisms, cooperative folding events between both peptide and MHCII help to stabilize the final folded structure.

Implicit in this model is the assumption that unfolding and peptide release proceeds in a similar manner. Indeed, this concept is supported by the cooperative effects observed in the dissociation rate ($t_{1/2}$) of multisubstituted complexes. For certain multiple substitutions, the $K_D$ of the complex was extremely high, precluding direct measurement of the dissociation rate. However, competition binding experiments allowed us to determine the extent to which these low affinity peptides can compete with HA for binding to the DR1 molecule. We interpret this level of competition as representative of a partial folding event which is highly cooperative despite the lack of stable complex formation. High levels of cooperativity in the absence of stable complex formation indicate the importance of the initial events in the folding process.

The change from the partially disordered state to the final stable complex corresponds to the phase transition associated with protein folding (*46*), which can be viewed as the sum of a number of partially folded states approaching a critical point at which there is an all-or-none conformational change. The modifications we make bring the complex closer to the transition point in an exponential manner as defined by the slope of cooperativity versus $t_{1/2}$ or $K_D$. The exact significance of the value obtained for the slope of the cooperativity is unclear. However, it may be related to the critical exponent associated with continuous phase transitions. It is obvious from the data that cooperativity increases the farther the complex is destabilized or at lower affinities. In a nucleation-based model, this would be expected, as the first few events

in folding, or the last few in unfolding, would be the most important.

We envisage that the structural changes that accompany peptide binding to MHCII in the endosome will be similar to those we have analyzed here. Nevertheless, our in vitro system does not address other important facets of the antigen presentation process in the endosome, such as the effect of planar membrane geometry, the binding of the invariant chain (*47*), and the activity of the peptide exchange factor, HLA-DM (*2*). Although the exact mechanism of the peptide exchange reaction catalyzed by HLA-DM remains unclear, kinetic studies suggest that it acts as a conformational catalyst (*48*). Thus, one might expect to observe cooperative effects on the peptide exchange reaction in the presence of HLA-DM. Such experiments could be very interesting tests of the folding hypothesis.

In all the experiments presented here, the primary hydrophobic anchor residues at P1, P4, P6, and P9 have been held constant. It will be important to test whether the cooperativity observed here for relatively solvent accessible residues will extend to the interactions at these major pocket sites. In our analysis, a substitution affecting a minor hydrophobic pocket interaction (P7) did show cooperativity. On this basis, we would expect that cooperativity would be observed in the major hydrophobic pocket/side chain interactions. Measurement of cooperative effects at these positions could increase the power of pocket-based epitope prediction algorithms.

A cooperative model of peptide/MHCII interactions changes how we view epitope selection via the MHCII pathway. First, in order to predict the outcome of epitope selection, we must consider how all contributions to binding energy impact the folding process. Second, all positions have to be considered. Third, a change in one position must be considered in the context of any other substitutions. In lieu of empirical matrix-based algorithms (*12*), epitope prediction based on calculating folding energies may provide for better vaccine design. Such approaches would also explain those instances in which epitope presentation occurs in the absence of any definable binding motifs or anchor/pocket interactions (*8*−*10*). Finally, cooperativity may reveal novel mechanisms of pathogen escape (*49*) at the level of MHCII binding, and help explain those instances of aberrant epitope presentation in the context of autoimmune disease (*50*).

## ACKNOWLEDGMENT

We thank Trudy Holyst for peptide synthesis, Laura Newman for help in generating $\beta$81 protein, and Dr. Lawrence Stern for DR1 expressing S2 cells, expression plasmids, and helpful discussions.

## REFERENCES

1. Watts, C., and Powis, S. (1999) Pathways of antigen processing and presentation, *Rev. Immunogenet. 1*, 60−74.
2. Brocke, P., Garbi, N., Momburg, F., and Hammerling, G. J. (2002) HLA-DM, HLA-DO and tapasin: functional similarities and differences, *Curr. Opin. Immunol. 14*, 22−29.
3. Nelson, C. A., and Fremont, D. H. (1999) Structural principles of MHC class II antigen presentation, *Rev. Immunogenet. 1*, 47−59.
4. Jardetzky, T. S., Gorga, J. C., Busch, R., Rothbard, J., Strominger, J. L., and Wiley, D. C. (1990) Peptide binding to HLA-DR1: a peptide with most residues substituted to alanine retains MHC binding, *EMBO J. 9*, 1797−1803.
5. O'Sullivan, D., Arrhenius, T., Sidney, J., del Guercio, M. F., Albertson, M., Wall, M., Oseroff, C., Southwood, S., Colon, S. M., Gaeta, F. C., and Sette, A. (1991) On the interaction of promiscuous antigenic peptides with different DR alleles. Identification of common structural motifs, *J. Immunol. 147*, 2663−2669.
6. Hammer, J., Takacs, B., and Sinigaglia, F. (1992) Identification of a motif for HLA-DR1 binding peptides using M13 display libraries, *J. Exp. Med. 176*, 1007−1013.
7. Buus, S. (1999) Description and prediction of peptide-MHC binding: the 'human MHC project', *Curr. Opin. Immunol. 11*, 209−213.
8. Scott, C. A., Peterson, P. A., Teyton, L., and Wilson, I. A. (1998) Crystal structures of two I-Ad-peptide complexes reveal that high affinity can be achieved without large anchor residues, *Immunity 8*, 319−329.
9. Liu, X., Dai, S., Crawford, F., Fruge, R., Marrack, P., and Kappler, J. (2002) Alternate interactions define the binding of peptides to the MHC molecule IA(b), *Proc. Natl. Acad. Sci. U.S.A. 99*, 8820−8825.
10. Carrasco-Marin, E., Kanagawa, O., and Unanue, E. R. (1999) The lack of consensus for I-A(g7)-peptide binding motifs: is there a requirement for anchor amino acid side chains?, *Proc. Natl. Acad. Sci. U.S.A. 96*, 8621−8626.
11. Anderson, M. W., and Gorski, J. (2003) Cutting edge: TCR contacts as anchors: effects on affinity and HLA-DM stability, *J. Immunol. 171*, 5683−5687.
12. Sturniolo, T., Bono, E., Ding, J., Raddrizzani, L., Tuereci, O., Sahin, U., Braxenthaler, M., Gallazzi, F., Protti, M. P., Sinigaglia, F., and Hammer, J. (1999) Generation of tissue-specific and promiscuous HLA ligand databases using DNA microarrays and virtual HLA class II matrices, *Nat. Biotechnol. 17*, 555−561.
13. Bian, H., Reidhaar-Olson, J. F., and Hammer, J. (2003) The use of bioinformatics for identifying class II-restricted T-cell epitopes, *Methods 29*, 299−309.
14. Sadegh-Nasseri, S., and Germain, R. N. (1992) How MHC class II molecules work: peptide-dependent completion of protein folding, *Immunol. Today 13*, 43−46.
15. Sundberg, E. J., and Mariuzza, R. A. (2000) Luxury accommodations: the expanding role of structural plasticity in protein-protein interactions, *Struct. Folding Des. 8*, R137−R142.
16. Jimenez, R., Salazar, G., Yin, J., Joo, T., and Romesberg, F. E. (2004) Protein dynamics and the immunological evolution of molecular recognition, *Proc. Natl. Acad. Sci. U.S.A. 101*, 3803−3808.
17. Dornmair, K., Rothenhausler, B., and McConnell, H. M. (1989) Structural intermediates in the reactions of antigenic peptides with MHC molecules, *Cold Spring Harbor Symp. Quant. Biol. 54*, Part 1, 409−416.
18. Sadegh-Nasseri, S., and McConnell, H. M. (1989) A kinetic intermediate in the reaction of an antigenic peptide and I-Ek, *Nature 337*, 274−276.
19. Sadegh-Nasseri, S., and Germain, R. N. (1991) A role for peptide in determining MHC class II structure, *Nature 353*, 167−170.
20. Sadegh-Nasseri, S., Stern, L. J., Wiley, D. C., and Germain, R. N. (1994) MHC class II function preserved by low-affinity peptide interactions preceding stable binding, *Nature 370*, 647−650.
21. Rabinowitz, J. D., Vrljic, M., Kasson, P. M., Liang, M. N., Busch, R., Boniface, J. J., Davis, M. M., and McConnell, H. M. (1998) Formation of a highly peptide-receptive state of class II MHC, *Immunity 9*, 699−709.
22. Schmitt, L., Boniface, J. J., Davis, M. M., and McConnell, H. M. (1999) Conformational isomers of a class II MHC-peptide complex in solution, *J. Mol. Biol. 286*, 207−218.
23. Natarajan, S. K., Assadi, M., and Sadegh-Nasseri, S. (1999) Stable peptide binding to MHC class II molecule is rapid and is determined by a receptive conformation shaped by prior association with low affinity peptides, *J. Immunol. 162*, 4030−4036.
24. Kasson, P. M., Rabinowitz, J. D., Schmitt, L., Davis, M. M., and McConnell, H. M. (2000) Kinetics of peptide binding to the class II MHC protein I-Ek, *Biochemistry 39*, 1048−1058.
25. Joshi, R. V., Zarutskie, J. A., and Stern, L. J. (2000) A three-step kinetic mechanism for peptide binding to MHC class II proteins, *Biochemistry 39*, 3751−3762.
26. Zarutskie, J. A., Sato, A. K., Rushe, M. M., Chan, I. C., Lomakin, A., Benedek, G. B., and Stern, L. J. (1999) A conformational change in the human major histocompatibility complex protein HLA-DR1 induced by peptide binding, *Biochemistry 38*, 5878−5887.

27. Sato, A. K., Zarutskie, J. A., Rushe, M. M., Lomakin, A., Natarajan, S. K., Sadegh-Nasseri, S., Benedek, G. B., and Stern, L. J. (2000) Determinants of the peptide-induced conformational change in the human class II major histocompatibility complex protein HLA-DR1, *J. Biol. Chem. 275*, 2165−2173.
28. Carven, G. J., Chitta, S., Hilgert, I., Rushe, M. M., Baggio, R. F., Palmer, M., Arenas, J. E., Strominger, J. L., Horejsi, V., Santambrogio, L., and Stern, L. J. (2004) Monoclonal antibodies specific for the empty conformation of HLA-DR1 reveal aspects of the conformational change associated with peptide binding, *J. Biol. Chem. 279*, 16561−16570.
29. Fersht, A. R. (1999) *Structure and Mechanism in Protein Science: a Guide to Enzyme Catalysis and Protein Folding*, W. H. Freeman, New York.
30. Fremont, D. H., Stura, E. A., Matsumura, M., Peterson, P. A., and Wilson, I. A. (1995) Crystal structure of an H-2Kb-ovalbumin peptide complex reveals the interplay of primary and secondary anchor positions in the major histocompatibility complex binding groove, *Proc. Natl. Acad. Sci. U.S.A. 92*, 2479−2483.
31. Latek, R. R., Petzold, S. J., and Unanue, E. R. (2000) Hindering auxiliary anchors are potent modulators of peptide binding and selection by I-Ak class II molecules, *Proc. Natl. Acad. Sci. U.S.A. 97*, 11460−11465.
32. McFarland, B. J., Katz, J. F., Beeson, C., and Sant, A. J. (2001) Energetic asymmetry among hydrogen bonds in MHC class II*peptide complexes, *Proc. Natl. Acad. Sci. U.S.A. 98*, 9231−9236.
33. Stern, L. J., Brown, J. H., Jardetzky, T. S., Gorga, J. C., Urban, R. G., Strominger, J. L., and Wiley, D. C. (1994) Crystal structure of the human class II MHC protein HLA-DR1 complexed with an influenza virus peptide, *Nature 368*, 215−221.
34. Stern, L. J., and Wiley, D. C. (1992) The human class II MHC protein HLA-DR1 assembles as empty alpha beta heterodimers in the absence of antigenic peptide, *Cell 68*, 465−477.
35. Jensen, P. E., Moore, J. C., and Lukacher, A. E. (1998) A europium fluoroimmunoassay for measuring peptide binding to MHC class I molecules, *J. Immunol. Methods 215*, 71−80.
36. Beeson, C., and McConnell, H. M. (1994) Kinetic intermediates in the reactions between peptides and proteins of major histocompatibility complex class II, *Proc. Natl. Acad. Sci. U.S.A. 91*, 8842−8845.
37. Creighton, T. E. (1995) Protein folding. An unfolding story, *Curr. Biol. 5*, 353−356.
38. Williams, D. H., Stephens, E., and Zhou, M. (2003) Ligand binding energy and catalytic efficiency from improved packing within receptors and enzymes, *J. Mol. Biol. 329*, 389−399.
39. Horovitz, A., and Fersht, A. R. (1990) Strategy for analysing the co-operativity of intramolecular interactions in peptides and proteins, *J. Mol. Biol. 214*, 613−617.
40. Horovitz, A., and Fersht, A. R. (1992) Co-operative interactions during protein folding, *J. Mol. Biol. 224*, 733−740.
41. Dessen, A., Lawrence, C. M., Cupo, S., Zaller, D. M., and Wiley, D. C. (1997) X-ray crystal structure of HLA-DR4 (DRA*0101, DRB1*0401) complexed with a peptide from human collagen II, *Immunity 7*, 473−481.
42. McFarland, B. J., Beeson, C., and Sant, A. J. (1999) Cutting edge: a single, essential hydrogen bond controls the stability of peptide-MHC class II complexes, *J. Immunol. 163*, 3567−3571.
43. Zavala-Ruiz, Z., Sundberg, E. J., Stone, J. D., DeOliveira, D. B., Chan, I. C., Svendsen, J., Mariuzza, R. A., and Stern, L. J. (2003) Exploration of the P6/P7 region of the peptide-binding site of the human class II major histocompatability complex protein HLA-DR1, *J. Biol. Chem. 278*, 44904−44912.
44. Zavala-Ruiz, Z., Strug, I., Anderson, M. W., Gorski, J., and Stern, L. J. (2004) A polymorphic pocket at the P10 position contributes to peptide binding specificity in class II MHC proteins, *Chem. Biol. 11*, 1395−1402.
45. Kumar, S., and Bansal, M. (1998) Dissecting alpha-helices: position-specific analysis of alpha-helices in globular proteins, *Proteins 31*, 460−476.
46. Privalov, P. L. (1979) Stability of proteins: small globular proteins, *Adv. Protein Chem. 33*, 167−241.
47. Sant, A. J., and Miller, J. (1994) MHC class II antigen processing: biology of invariant chain, *Curr. Opin. Immunol. 6*, 57−63.
48. Zarutskie, J. A., Busch, R., Zavala-Ruiz, Z., Rushe, M., Mellins, E. D., and Stern, L. J. (2001) The kinetic basis of peptide exchange catalysis by HLA-DM, *Proc. Natl. Acad. Sci. U.S.A. 98*, 12450−12455.
49. McMichael, A. (1998) T cell responses and viral escape, *Cell 93*, 673−676.
50. He, X. L., Radu, C., Sidney, J., Sette, A., Ward, E. S., and Garcia, K. C. (2002) Structural snapshot of aberrant antigen presentation linked to autoimmunity: the immunodominant epitope of MBP complexed with I-Au, *Immunity 17*, 83−94.
51. Hennecke, J., Carfi, A., and Wiley, D. C. (2000) Structure of a covalently stabilized complex of a human alphabeta T-cell receptor, influenza HA peptide and MHC class II molecule, HLA-DR1, *EMBO J. 19*, 5611−5624.
52. Guex, N., and Peitsch, M. C. (1997) SWISS-MODEL and the Swiss-PdbViewer: an environment for comparative protein modeling, *Electrophoresis 18*, 2714−2723.
53. De Lano, W. L. (2002) *The PyMOL Molecular Graphics System*, De Lano Scientific, San Carlos, CA.

BI048675S